USE OF 3-D CORTICAL MORPHOMETRY FOR MAPPING INCREASED CORTICAL GYRIFICATION AND COMPLEXITY IN WILLIAMS SYNDROME

D. Tosun[1], *A. L. Reiss*[2], *A. D. Lee*[1], *R. A. Dutton*[1], *J. A. Geaga*[1], *K. M. Hayashi*[1], *M. A. Eckert*[2], *U. Bellugi*[3], *A. M. Galaburda*[4], *J. R. Korenberg*[5], *D. L. Mills*[6], *A W. Toga*[1], *P. M. Thompson*[1]

[1] Laboratory of Neuro Imaging, Brain Mapping Division, Dept. of Neurology, UCLA School of Medicine, Los Angeles, CA 90095, USA
[2] Center for Interdisciplinary Brain Sciences Research, Department of Psychiatry and Behavioral Sciences, Stanford University School of Medicine, Stanford, CA 94305, USA
[3] Salk Institute Laboratory for Cognitive Neuroscience, La Jolla, CA 92037, USA
[4] Harvard Medical School Department of Neurology, Boston, MA 02215, USA
[5] UCLA Department of Pediatrics, Los Angeles, CA 90095, USA
[6] Emory University, Department of Psychology, Atlanta, GA 30322, USA

ABSTRACT

In this paper, we describe the use of three different shape measures — i.e., shape index, curvedness, and L_2 norm of mean curvature — to quantify cortical gyrification and complexity, thereby evaluating brain structural differences between individuals with Williams syndrome (WS) and healthy controls. Unlike traditional measures of gyrification, the proposed measures analyze the intrinsic geometry of the cortex in three-dimensional (3-D) space. We analyzed the local and global cortical folding patterns of 39 WS and 39 controls using these shape measures, showing increased gyrification in the cingulate, visual cortex, superior parietal lobule, and central sulcus regions (more pronounced in the left brain hemisphere), and increased cortical complexity in left temporal and left parietal lobes in WS. These findings agree with, and extend, previously published studies and may relate to the characteristic clinical and cognitive profiles of individuals with WS.

1. INTRODUCTION

Research on diagnostic imaging modalities such as magnetic resonance (MR) imaging has led to the use of computers to noninvasively extract anatomic and physiological information to understand the neurobiology of brain development and disease. Brain imaging is of particular interest in studying WS, a rare developmental disorder associated with a genetic deletion of approximately 1 to 2 Mb in the 7q11.23 chromosomal region [1]. WS is characterized by disrupted cortical development and mild to moderate mental retardation but relative proficiencies in language skills, social drive, and musical ability [1]. Findings from *post mortem* and *in vivo* studies on WS include structural deviations in terms of brain volume and shape [2, 3], volumetric and tissue-specific asymmetries [4, 3], and increases in global cortical complexity as well as regional gyrification [2, 5].

The work presented in this paper is motivated by the need for automated and robust cortical morphometry analysis techniques to quantify the impact of altered gene expression on cortical development, particularly on cortical gyrification, which is disturbed in WS. Traditionally, measures from two dimensional (2-D) cross-sections are used to quantify cortical gyrification [6, 2]. Analysis based on these 2-D measures not only depends on brain orientation and the direction of image slicing, but may be limited by the accuracy and speed of raters in manual tracing. Recent advances in reconstructing cortical surfaces from 3-D MR brain image volumes [7, 8, 9] have led to the development of techniques to analyze cortical complexity in 3-D, often focusing on subregions (e.g.,., lobes) of the cortex. A unique approach based on shape analysis of 3-D cortical surface models was proposed in [5, 10] to assess both local and global sulcal/gyral complexity of the cortex by analyzing its 3-D intrinsic surface geometry. This approach both addresses the issues with previous measures utilized to quantify the cortical gyrification and provides dense estimates of degree of cortical folding throughout the cortical surface.

In this paper, inspired by the work presented in [5, 10], we describe the use of other measures to quantify cortical complexity and thereby identify and localize brain structure differences between individuals with WS and controls. First, we introduce two local shape measures — i.e., shape index and curvedness — to analyze the sulcal/gyral pattern of cortex in terms of *shape* and *size*, separately. These measures are defined at every point of the cortical surface model yielding a dense (i.e., local) analysis of cortical gyrification. Second, we introduce a global shape measure to quantify the folding com-

Supported by grants R21 EB01651, R21 RR019771, AG016570, K02 MH01142, R01 HD31715, P01 HD33113, and U54 RR021813 .

plexity of specific cortical subregions — e.g., lobes. Then, we present our empirical findings using these measures to assess structural differences between WS and control subject brains.

2. METHOD

Data Set. A total of 39 subjects with genetically confirmed WS (29.9 $\pm$ 8.9 years of age; 17 males and 22 females) and 39 age-matched controls (27.1 $\pm$ 7.6 years of age; 16 males and 23 females) were analyzed in this study. All WS participants (who had no history of epilepsy or other neurological conditions) were evaluated at the Salk Institute as part of a program project on genetics, neuroanatomy, neurophysiology, and cognition. Control subjects (with no history of major psychiatric, neurological, or cognitive impairment) were recruited at both the Salk Institute and Stanford University [3]. Data were acquired on a GE Signa 1.5 Tesla MR scanner using a T1-weighted spoiled gradient echo (SPGR) pulse sequence with the following parameters: TE = 5 ms; TR = 24 ms; 45° flip angle; matrix size = 256 $\times$ 192; FOV = 240 mm $\times$ 240 mm; slice thickness = 1.2 mm, with 124 contiguous slices.

Cortical Surface Reconstruction and Spatial Normalization. The first processing step was to remove nonbrain tissue (i.e., scalp, orbits, etc.) from the 3-D MR image volumes followed by the affine transformation of the remaining image volume into the standard space of the International Consortium for Brain Mapping-53 (ICBM-53) average brain [11]. Then each individual's cortical surface was extracted using an automated software [7] yielding a spherical cortical surface coordinate system. Each resulting cortical surface was represented as a triangle mesh comprised of 65,536 mesh nodes. To empower the group analysis presented in this paper, we used a surface-based 3-D cortical warping technique driven by manually identified anatomical curves [12]. Using this method, we warped corresponding hemispheres of 78 subjects to each other and also warped the left and right cortical hemisphere of each subject to each other. This process smoothly reparameterizes each cortex such that the major sulcal curve landmarks in the cortex are placed at the same coordinate locations across all 78 subjects. Detailed descriptions of these processing steps can be found in [5].

Local Shape Measures to Analyze Sulcal/Gyral Folding Patterns. To help identify developmental differences between individuals with WS and controls, we require tools to analyze the geometry of the cortical surface — i.e., analyze the cortical folding pattern. The two principal curvatures κ_1 and κ_2, where $\kappa_1 \leq \kappa_2$, have the necessary information to fully describe the local shape of any given surface. However, curvature-based analysis of the folding pattern requires individual measures that possess a coordinate independent *geometrical* meaning such that the *shape* of the surface can be specified independent of the *size*. The widely used Gaussian and mean curvature measures, by themselves, fail to capture the intuitive notion of local shape very well. In particular, the Gaussian curvature vanishes both at planar points (i.e., $\kappa_1 = \kappa_2 = 0$), and at parabolic points (i.e., $\kappa_1 \neq 0$ and $\kappa_2 = 0$), thereby failing to distinguish these two shapes.

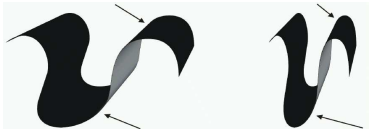

Fig. 1. Illustration of how SI and C measures complement each other in defining the local surface *shape* and the *size*.

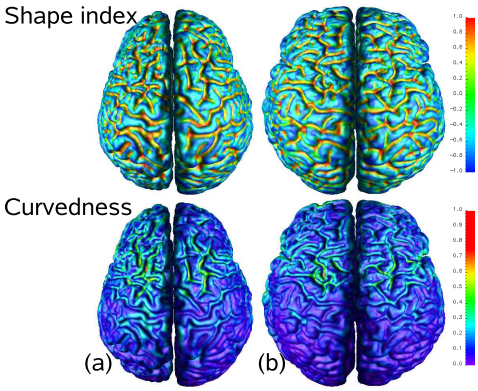

Fig. 2. Shape measures for (a) an individual with WS and (b) a healthy control.

In [13], *shape index* and *curvedness* measures were introduced as a pair of local shape indicator measures. The shape index, SI, and the curvedness, C, are defined as

$$\mathrm{SI} = \frac{2}{\pi} \arctan \frac{\kappa_2 + \kappa_1}{\kappa_2 - \kappa_1}, \quad \mathrm{C} = \sqrt{\frac{\kappa_1^2 + \kappa_2^2}{2}}. \tag{1}$$

SI specifies the local surface geometry up to a scaling factor (i.e., similarity), and takes values in $[-1, +1]$. The extreme values of SI represent local shapes that look like either the inside ($\mathrm{SI} = -1$) or the outside ($\mathrm{SI} = 1$) of a spherical surface, and intermediate values correspond to the local surface shapes observed when these shapes smoothly morphed one to the other. In contrast, C is inversely proportional to the *size* of the surface patch. Therefore, unlike the Gaussian and mean curvature measures, SI and C measures complement each other in defining the local surface *shape* and *size*. This is made clear by referring to Fig. 1 where the two synthetic shapes have the same SI value at the local geometry pointed out by arrows while relatively narrower folds in the second shape possess larger C values.

Figs. 2(a) and (b) show SI and C measures for a sample individual with WS and a sample control, respectively. The SI successfully distinguishes the cortical features such as sulci and gyri and C gives the intensity of the folding. One can also see that C is relatively larger in the individual with WS.

Global Shape Measure to Quantify Complexity of Cortical Subregions. A global measure that quantifies the complexity of the surface and allows group analysis should be

scale-invariant to capture information about the shape of the surface. Our global shape measure is based on the L_2 norm of mean curvature, $\|H\|_2$ [14], which is defined as

$$\|H\|_2 = \sqrt{\frac{1}{4\pi}\int H^2 dA}\,, \qquad (2)$$

where H is the mean curvature. The measure $\|H\|_2$ is approximated by discrete differential geometry operators [14]. This is a global measure of extrinsic geometry, and is minimal for a sphere of arbitrary radius — i.e., $\|H\|_2 = 1$. $\|H\|_2$ gets larger as the degree of surface folding increases.

3. RESULTS AND DISCUSSION

Cortical Gyrification. Local shape measure maps — i.e., SI and C — were computed for 39 individuals with WS and 39 controls. The shape measure maps were smoothed by averaging in a geodesic neighborhood of radius 20 mm. Then, we calculated group means for each scalar measure at each node of mesh model in ICBM space. The mean difference between shape measure maps of WS and controls, mapped on an averaged surface mesh model in ICBM space, are shown in Figs. 3(a) and (c), and the regions with significant mean difference are highlighted in Figs. 3(b) and (d). An increased SI measure indicates a difference in folding pattern — i.e., shift to a more convoluted surface. The WS group had increased convolution in the left anterior cingulate, paracentral, central sulci and right precentral and superior temporal gyri. Increases in the size of sulcal/gyral foldings were observed as increased C values in WS group. These regions include most of the medial surface of the left hemisphere — i.e., the anterior and posterior cingulate, paracentral, superior rostral, parieto-occipital, and posterior calcarine — as well as the left central, left/right transverse occipital, and right parieto-occipital cortex. The increase in both the degree of folding and size of folding in WS is interpreted as a difference in cortical gyrification between groups.

Both the shape and size differences between groups are visually more pronounced in the left hemisphere. In order to elucidate this hemispheric asymmetry, we calculated a lateralization index for the curvedness measure using the formula (R-L)/0.5(R+L) for the right cortical hemisphere and (L-R)/0.5(R+L) for the left cortical hemisphere so that positive values indicate an asymmetry with greater values in that hemisphere. We set the lateralization index to zero on both hemispheres if the calculated value was negative, followed by calculation of the mean differences in lateralization index between WS and controls. The regions showing significant mean difference in the lateralization index are shown in Fig. 3(e). WS subjects show leftward asymmetry throughout the medial surface — e.g., posterior and anterior cingulate, and visual cortex — with diminished rightward asymmetry in the anterior cingulate region. We also observe a leftward asymmetry in the left central sulcus region in WS subjects. These increased gyrification and lateralization findings corroborate previously published work [4, 2, 5], encouraging further investigation of the proposed measures in quantifying cortical gyrification in related neuroanatomy studies.

Cortical Complexity. The second analysis we carried out aimed to compare the cortical complexity of WS and controls. Each subject's cortical surface model was partitioned into four lobes — i.e., frontal, occipital, parietal, and temporal lobes of left and right hemispheres — using an atlas based method (see [5] for details). Then, we computed the global shape measure $\|H\|_2$ on the partitioned lobes, yielding a surface complexity measure for each lobe. The mean surface complexity for each lobe was calculated for WS and controls, separately. Each lobe's mean surface complexity appeared larger — i.e., more convoluted surface — in left hemisphere compared to right hemisphere for both groups, however, the difference was significantly ($P < 0.05$) only for occipital lobes in WS group. Similarly, we found that the mean surface complexity for the lobes was consistently higher in WS compared to controls. Only left temporal and parietal lobes were significantly ($P < 0.05$) more complex in WS than controls. Future studies at the genetic and cognitive level are required to understand how these regional alterations may relate to the behavioral and physiological differences in WS. However, by identifying the scope of these cortical anomalies, the impact of the genetic deletion in WS will be better established.

4. REFERENCES

[1] J. R. Korenberg, X. N. Chen, H. Hirota, Z. Lai, U. Bellugi, D. Burian, B. Roe, and R. Matsuoka, "Genome structure and cognitive map of Williams syndrome," *J. Cognitive Neuroscience*, vol. 12, pp. S89–S107, 2000.

[2] J. E. Schmitt, K. Watts, S. Eliez, U. Bellugi, A. M. Galaburda, and A. L. Reiss, "Increased gyrification in Williams syndrome: evidence using 3D MRI methods," *Dev Med Child Neurol.*, vol. 44, no. 5, pp. 292–295, 2002.

[3] A. L. Reiss, M. A. Eckert, F. E. Rose, A. Karchemskiy, S. Kesler, M. Chang, M. F. Reynolds, H. Kwon, and A. Galaburda, "An experiment of nature: brain anatomy parallels cognition and behavior in Williams syndrome," *J. Neuroscience*, pp. 5009–5015, 2004.

[4] A. M. Galaburda and U. Bellugi, "Multi-level analysis of cortical neuroanatomy in Williams syndrome," *J. Cognitive Neuroscience*, vol. 12, pp. S74–S88, 2000.

[5] P. M. Thompson, A. D. Lee, R. A. Dutton, J. A. Geaga, K. M. Hayashi, M. A. Eckert, U. Bellugi, A. M. Galaburda, J. R. Korenberg, D. L. Mills, A. W. Toga, and A. L. Reiss, "Abnormal cortical complexity and thickness profiles mapped in Williams syndrome," *J. Neuroscience*, pp. 4146–4158, 2005.

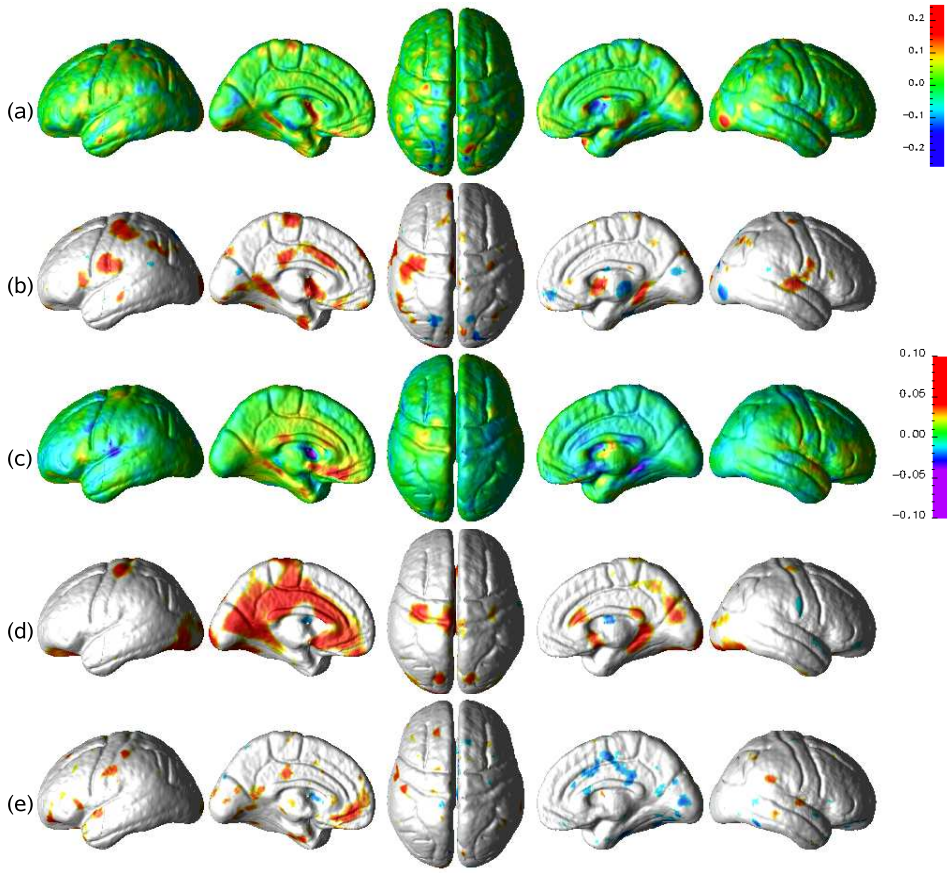

Fig. 3. Mean group differences are shown for (a) the shape index map and (c) the curvedness map (WS - Controls); Regions with a significant mean difference ($P < 0.05$, corrected for multiple comparisons using False Discovery Rate (FDR) [15]) for (b) shape index and (d) the curvedness measures; (e) Mean difference in the lateralization of the curvedness maps (color coding for significance maps: WS $>$ Controls colored in red/yellow and Controls $>$ WS colored in blue/cyan.

[6] K. Zilles, E. Armstrong, A. Schleicher, and H. Kretschmann, "The human pattern of gyrification in the cerebral cortex," *Anatomy and Embryology*, vol. 179, pp. 173–179, 1988.

[7] D. MacDonald, N. Kabani, D. Avis, and A. Evans, "Automated 3D extraction of inner and outer surfaces of cerebral cortex from MRI," *NeuroImage*, vol. 12, no. 3, pp. 340–356, 2000.

[8] A. M. Dale, B. Fischl, and M. I. Sereno, "Cortical surface-based analysis I: Segmentation and surface reconstruction," *NeuroImage*, vol. 9, no. 2, pp. 179–194, 1999.

[9] X. Han, D. L.Pham, D. Tosun, M. E. Rettmann, C. Xu, and J. L. Prince, "CRUISE: Cortical reconstruction using implicit surface evolution," *NeuroImage*, vol. 23, no. 3, pp. 997–1012, 2004.

[10] E. Luders, P. M. Thompson, K. L. Narr, A. W. Toga, L. Jancke, and C. Gaser, "A curvature-based approach to estimate local gyrification on the cortical surface," *NeuroImage*, 2005.

[11] J. C. Mazziotta, A. W. Toga, A. Evans, P. Fox, and J. Lancaster, "A probabilistic atlas of the human brain: Theory and rationale for its development," *NeuroImage*, vol. 2, pp. 89–101, 1995.

[12] P. M. Thompson and A. W. Toga, "A surface-based technique for warping three-dimensional images of the brain," *IEEE Trans. Medical Imaging*, vol. 15, pp. 402–417, 1996.

[13] J. J. Koenderink and A. J. van Doorn, "Surface shape and curvature scales," *Image and Vision Computing*, vol. 10, no. 8, pp. 557–565, 1992.

[14] D. Tosun, M. E. Rettmann, and J. L. Prince, "Mapping techniques for aligning sulci across multiple brains," *Medical Image Analysis - Special issue: Medical Image Computing and Computer-Assisted Intervention - MICCAI 2003 - Edited by R. Ellis and T. Peters*, vol. 8, no. 3, pp. 295–309, 2004.

[15] Y. Benjamini and Y. Hockberg, "Controlling the false discovery rate: a practical and powerful approach to mltiple testing," *J. Royal Statistical Society*, 1995.